

A FIRST EGRET-UNID-RELATED AGENDA FOR THE NEXT-GENERATION CHERENKOV TELESCOPES

Dirk Petry

Dept. of Physics and Astronomy

Iowa State University

Ames, IA 50011

petry@iastate.edu

Keywords: Cherenkov Telescopes, Unidentified Gamma-Ray Sources, Very-High-Energy Gamma-Rays

Abstract The next generation of Imaging Atmospheric Cherenkov Telescopes (IACTs) will open the regime between ≈ 30 GeV and 200 GeV to ground-based gamma observations with unprecedented point source sensitivity and source location accuracy. I examine the prospects of observing the unidentified objects (UNIDs) of the Third EGRET Catalog using the IACT observatories currently under construction by the CANGAROO, HESS, MAGIC and VERITAS collaborations. Assuming a modest spectral steepening similar to that observed in the inverse Compton component of the Crab Nebula spectrum and taking into account the sensitivity of the instruments and its zenith angle dependence, a detailed list of 78 observable objects is derived which is then further constrained to 38 prime candidates. The characteristics of this agenda are discussed.

1. INTRODUCTION

The EGRET experiment (1991-1999) has given us the first detailed view of the entire high-energy gamma-ray sky. Its successful history is described by other authors (e.g. D.J. Thompson, these proceedings). In parallel with EGRET's observations, observers also began to explore the gamma-ray sky at even higher energies. The first successful observation of a gamma-ray source above 500 GeV (the Crab Nebula, Weekes et al. 1989) using a Cherenkov telescope was made only few years before EGRET's launch and one year after it followed the detection of the second source, Mkn 421 (Punch et al. 1992). Both sources were also

detected by EGRET and it has become common practice to show the EGRET flux measurement as a reference in plots of Cherenkov telescope flux measurements.

However, it soon became clear that an EGRET detection did not imply that the source would also be detected at very high energies. The class of EGRET Blazars has been thoroughly observed by Cherenkov telescopes, but none has been detected except Mkn 421 although extrapolations of the EGRET spectra are in many cases comfortably above the point source sensitivity of the present instruments. The second extragalactic source ever to be detected at very high energies, Mkn 501, was initially not an EGRET source. Only by raising the energy threshold and looking for flares, Kataoka et al. (1999) were able to report a marginal detection. Today, the situation remains essentially the same. About 11 very high energy (VHE) gamma-ray sources have been detected: 4 Blazars (Mkn 421, Mkn 501, 1ES2344+514, PKS2155-304) and 7 SNRs/Plerions (Crab Nebula, PSR1706-44, SN1006, Cas A, Vela, PSR B1509-58, SNR 347.3-00.5) (see figure 1). About half of these are EGRET sources.

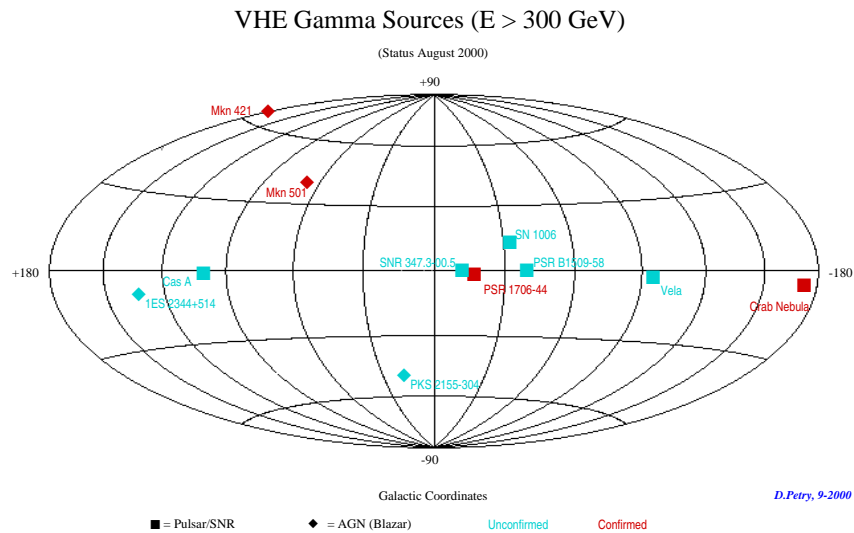


Figure 1 A sky map of the presently known VHE gamma-ray sources.

We are therefore looking at three classes of very high energy sources: (a) steeply cutting-off sources which are detected by EGRET but become unobservable above a few 100 GeV, (b) flat spectrum sources like Mkn 501 which only become observable at higher energies, and (c) in-

intermediate cases like Mkn 421 or the Crab Nebula. Most known sources must belong to type (a) given the way observation technology has developed. Whether this is really a selection effect is unclear. It seems that the universe becomes abruptly very much darker above a few 100 GeV. The number of detectable sources decreases rapidly with rising energy threshold even though the point source sensitivity of present Cherenkov telescopes is sufficiently many orders of magnitude better than that of EGRET to allow for a spectral index of 2.1 in differential photon flux. In other words, the cut-off of most high-energy source spectra seems to take place in the range 1 - 200 GeV. The first decade of energy in this range has been covered by EGRET and 57 sources have been detected (Lamb & Macomb 1997). The remaining 10-200 GeV have never been explored until today and it is this “gap” that forms the major incentive behind the projects for future, more sensitive Cherenkov telescopes.

According to the Third EGRET Catalog (Hartman et al. 1999), 197 out of the 271 objects in the catalog could so far not be identified with an optical, radio or X-ray counterpart with certainty. These sources are the Unidentified EGRET objects (UNIDs), 38 of which have already a tentative identification. The main reason for the non-identification of so many sources is the fact that their position is only poorly known because of EGRET’s wide point spread function and difficulties with modeling the background gamma radiation in the galactic plane (see again Thompson, these proceedings).

For EGRET, the point spread function is described by the angle θ_{68} , the half-opening angle of a cone which contains 68 % of all spark chamber events caused by photons from one point-source. This angle is weakly energy dependent. It is 5.85° at 100 MeV and 1.7° at 1 GeV. The expected accuracy of the source location is estimated by θ_{68}/\sqrt{N} where N is the number of detected photons. However, due to systematic errors of the background model also stronger sources can have location errors of more than 1° .

Imaging Atmospheric Cherenkov Telescopes (IACTs) are ground-based detectors using the atmosphere as a tracker and calorimeter. They typically have point spread functions with $\theta_{68} < 0.16^\circ$. The number of detected primary gamma-photons is typically > 100 . Hence source locations with arcminute accuracy are possible whenever a source can be detected. This has already been demonstrated by several authors (see the examples in figures 2 a and b). The possibility of separating two nearby point-sources is demonstrated by figure 2 (b): Two sources can be separated if their angular distance is $> 3\theta_{68}$. Cherenkov telescopes therefore seem to be the adequate tool for improving the source location of EGRET sources.

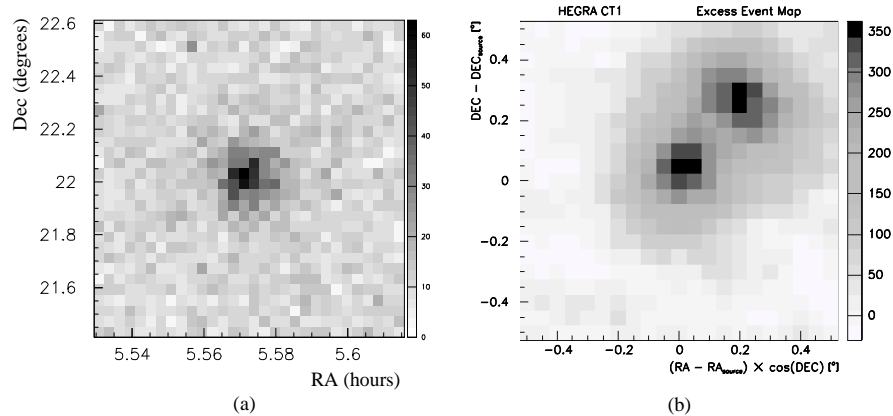


Figure 2 Point source location and separation with Cherenkov telescopes: (a) Excess event map of the region around the Crab Nebula obtained by Pühlhofer et al. (1997) using the HEGRA System of Cherenkov telescopes. The theoretical accuracy of the location is 0.01° . The reconstructed position deviates from the radio position of the Crab Nebula by 0.01° . (b) Excess event map of a hypothetical double source obtained by superimposing on- and 0.3° -off-axis observations of the Blazar Mkn 501 using the HEGRA CT1 Cherenkov telescope (Petry 1997). The point spread function of CT1 is $\theta_{68} = 0.1^\circ$ resulting in an expected location accuracy of 0.01° degrees. Taking into account a systematic tracking error of 0.1° , the position of Mkn 501 is correctly reconstructed from the on-axis observation. More important, the 0.3° angular distance between the two sources, which should be unaffected by the tracking error, is also correctly reconstructed within the expected 0.01° .

With their high photon statistics due to their large collection areas (typically 10^4m^2 at the threshold rising up to 10^5m^2 at larger zenith angles and higher energies) IACTs can also find pulsed emission and resolve fast time structures. This may be especially helpful since young pulsars (Kaaret & Cottam 1996) and Geminga-like radio-quiet pulsars (Yadigaroglu & Romani 1995) are among the candidate sources behind EGRET UNIDs.

In this article, I would like to explore what the next generation of IACTs with their improved sensitivity and lower energy threshold can achieve in terms of helping to identify the EGRET UNIDs. The result will mainly be a list of catalog objects for which observations with the new IACTs make sense and for which an identification can be expected. This defines their possible contribution to the solution of the EGRET UNID puzzle. As discussed in the next section, I will limit myself to the projects for IACTs with energy thresholds below 100 GeV. However, the exercise can easily be repeated for other experiments.

2. THE NEXT-GENERATION CHERENKOV TELESCOPES

Since the middle of the past decade, projects are underway to further improve the Cherenkov telescope technology and explore the 10-200 GeV regime with ground-based instruments. At the same time, the new telescopes are aiming to reach much improved sensitivity at higher energies.

In this article, I limit myself to those projects which use *imaging* atmospheric Cherenkov telescopes (IACTs), mostly because it has already been demonstrated that this technology can reach high flux sensitivity and high accuracy in determining source positions. I would like to mention, however, that other technologies are under development which may become competitive at some point, especially the non-imaging experiments using mirror arrays of former solar power plants (CELESTE (e.g. Smith et al. 1998), GRAAL (e.g. Arqueros et al. 1999), STACEE (e.g. Oser et al. 1999), Solar II (e.g. Zweerink et al. 1999) and the large-field-of-view, large-duty-cycle observatories MILAGRO (e.g. McCullough et al. 1999) and ARGO (not yet operational, see e.g. D’Ettore et al. 1999).

Table 1 The four projects for next-generation Imaging Cherenkov Telescopes

Project name	latitude	longitude	altitude	CTs ^a	$E_{\text{thr}}(0^\circ)^b$
CANGAROO III	31° S	137° E	160 m	4 × 10 m	80 GeV
HESS I	23° S	17° E	1800 m	4 × 13 m	40 GeV
MAGIC I	29° N	17° W	2200 m	1 × 17 m	30 GeV
VERITAS	32° N	111° W	1300 m	7 × 10 m	60 GeV

^aNumber of individual telescopes and diameter of their mirror dish.

^bPredicted energy threshold for gammas at zenith angle $\vartheta = 0^\circ$.

The next-generation projects for IACTs which will reach thresholds below 100 GeV are CANGAROO III (e.g. Mori et al. 1999), HESS I (e.g. Hofmann et al. 1999), MAGIC I (e.g. Lorenz et al. 1999) and VERITAS (e.g. Krennrich et al. 1999). The locations of the sites chosen for these observatories and their estimated minimum energy thresholds are given in table 1. The locations are also shown in figure 3. The roman numbers behind some of the project names denote the project phases.

All four experiments except CANGAROO III have published detailed Monte Carlo studies and presented a sensitivity curve. Figure 4 shows these sensitivity curves in the relevant energy range up to 1 TeV. CANGAROO III will reach a performance roughly similar to VERITAS (Mori 2001). The sensitivity curves show the integral gamma-ray flux which

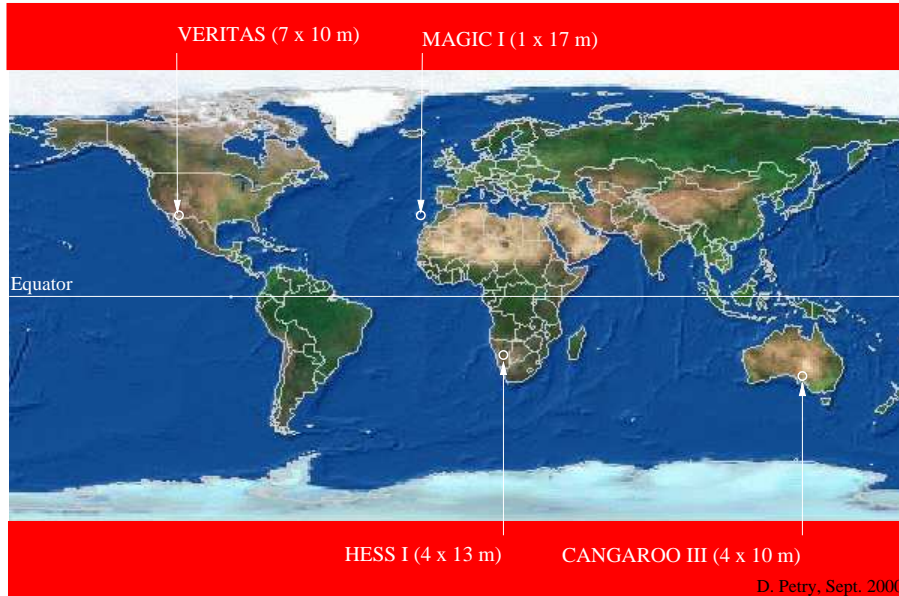


Figure 3 A world map indicating the locations of the four Imaging Atmospheric Cherenkov Telescope projects which may significantly contribute to the identification of EGRET UNIDs. See text for references.

the corresponding instrument can detect above the energy threshold E_0 with 20 % statistical error within an observation time of 50 h at small zenith angles. Also shown is the EGRET flux sensitivity for an observation time of 1 month taking into account the fact that the field of view and the duty cycle of EGRET is larger than that of an IACT.

Furthermore, figure 4 indicates in which flux regime the bulk part of the EGRET unidentified objects (UNIDs) would be found if their spectrum would continue as a straight power law from the 100 MeV, at which it is measured by EGRET, to 100 GeV. Plotting the distribution of the logarithms of the extrapolated fluxes at 100 GeV gives a nicely symmetric, nearly Gaussian distribution with an average of -10.79 corresponding to $1.6 \times 10^{-11} \text{ cm}^{-2}\text{s}^{-1}$ and a standard deviation of 1.2. The dashed lines in figure 4 outline the flux regime one standard deviation above and below this average.

3. OBSERVABILITY CRITERIA

Figure 4 is misleading as far as the actual observability of EGRET UNIDs by the IACTs under consideration is concerned. There are four

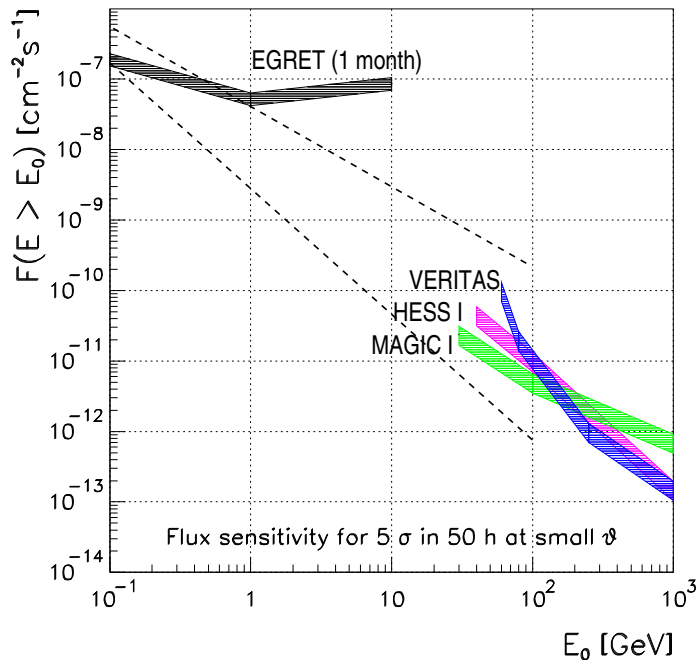


Figure 4 The sensitivity of HESS I, MAGIC I and VERITAS projects as given in Hofmann et al. (1999), Barrio et al. (1998) and Krennrich et al. (1999) respectively. Also shown is the EGRET sensitivity for one month of observing time. The dashed lines indicate the boundaries of the flux regime in which the central 68 % of the EGRET unidentified sources can be found if their 100 MeV fluxes are extrapolated to 100 GeV using the spectrum measured by EGRET.

aspects which have to be taken into account in assembling an observation agenda. These are discussed in the following.

3.1. SPECTRAL STEEPENING

The most obvious problem is that most EGRET sources will show spectral breaks above 100 MeV and the naive extrapolation of the power-law measured at around 100 MeV may be orders of magnitude above the real flux at the IACT threshold.

In order to predict observability more reliably, a certain spectral steepening has to be assumed. At the same time, no bias should be introduced towards any source class. As a first general approach, I will therefore assume a spectral steepening similar to that of the Crab Nebula which

is the best studied high energy gamma source. This is also adequate since most of the EGRET UNIDs are expected to be galactic such that cut-offs due to the absorption in the intergalactic infrared background should not be assumed a priori.

The differential spectral index $\gamma_{0.1}$ of the Crab Nebula at 0.1 GeV is given in the Third EGRET Catalog as $\gamma_{0.1} = 2.19 \pm 0.02$ while it is measured by the Whipple telescope at 500 GeV to be $\gamma_{500} = 2.49 \pm 0.06 \pm 0.04$ (Hillas et al. 1998). However, since the EGRET energy range is situated at the transition of the synchrotron component to the Inverse-Compton (IC) component of the Crab spectrum, the index 2.19 is actually an interpolation between the steep synchrotron spectrum and the beginning flat IC spectrum (de Jager et al. 1996). Above 1 GeV, the IC component is dominant. Hillas et al. (1998) show that the steepening of the IC component towards higher energies can be described by an increase in spectral index of 0.15 per decade of energy.

Applied to the extrapolation of the EGRET UNID spectra, this would mean that the integral flux above the energy x [GeV], $10 < x < 1000$ can roughly be expected to be

$$\begin{aligned}
 F(E > x[\text{GeV}]) &= F_0 \cdot 10^{-\alpha} \cdot 10^{-(\alpha+0.15)} \cdot \left(\frac{x}{10}\right)^{-(\alpha+0.30)} \\
 &= F_0 \cdot 10^{-(\alpha-0.15)} \cdot x^{-(\alpha+0.30)} \\
 &\quad \text{for } 10 < x < 100 \\
 \\
 F(E > x[\text{GeV}]) &= F_0 \cdot 10^{-\alpha} \cdot 10^{-(\alpha+0.15)} \cdot 10^{-(\alpha+0.30)} \cdot \left(\frac{x}{100}\right)^{-(\alpha+0.45)} \\
 &= F_0 \cdot 10^{-(\alpha-0.45)} \cdot x^{-(\alpha+0.45)} \\
 &\quad \text{for } 100 < x < 1000
 \end{aligned}
 \tag{1.1}$$

where F_0 is the integral flux above 0.1 GeV of a given source taken from the Third EGRET Catalog and α is the integral spectral index derived by subtracting 1.0 from the differential spectral index stated in the same catalog. E.g. for $\alpha = 1.0$, the steepening leads to an extrapolated integral flux at 100 GeV which is smaller by a factor 2.8 than the extrapolation without steepening.

3.2. SKY ACCESS LIMITS

Due to the decaying optical quality of the atmosphere towards larger zenith angles (water vapor, aerosols, background light from towns etc.), Cherenkov telescopes typically cannot observe at zenith angles much larger than 70° . And even if they can, they will not give priority to observations of objects which can only be observed at zenith angles larger than this.

The zenith angle ϑ at the upper culmination of an astronomical object depends on the the latitude ϕ of the observatory and the declination DEC of the object according to $\vartheta = |\phi - \text{DEC}|$. Hence the condition

$$|\phi - \text{DEC}| < 70^\circ \quad (1.2)$$

has to be imposed in the selection of observable objects. In order to make sure that the objects can be observed for sufficient time at $\vartheta < 70^\circ$, the permitted declination-range has to be narrowed down to $|\phi - \text{DEC}| < 60^\circ$ for objects which are not circumpolar. For the four projects under consideration these conditions mean

CANGAROO III	DEC	$< +29^\circ$	
HESS I	DEC	$< +37^\circ$	
MAGIC I	$-31^\circ <$	DEC	(1.3)
VERITAS	$-28^\circ <$	DEC	

Figure 5 shows the DEC distributions for the identified, tentatively identified and unidentified EGRET objects in the third catalog. The figure also indicates the DEC constraints for the four IACT projects. Due to the position of the galactic plane, the projects on the southern hemisphere clearly have better access to EGRET UNIDs. The distributions of identified and tentatively identified objects are nearly symmetrical.

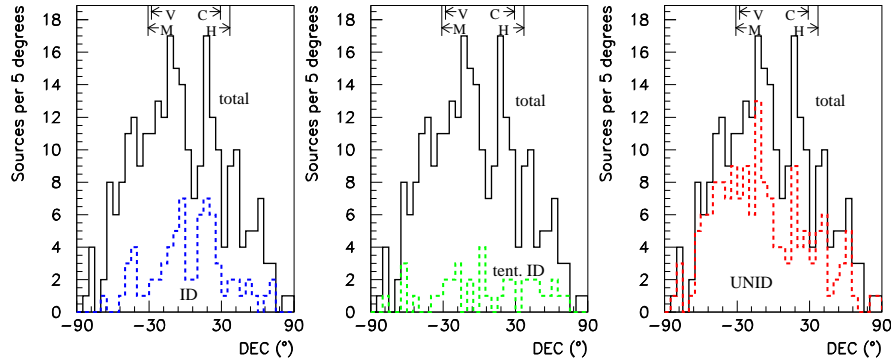


Figure 5 The distributions of the declination (DEC) of the objects in the third EGRET catalog. Left: the identified objects. Middle: the tentatively identified objects. Right: the unidentified objects. On all plots the distribution for the total number of sources is superimposed. At the top of each plot, arrows indicate the sky access limits of CANGAROO III (C), HESS I (H), MAGIC I (M) and VERITAS (V).

3.3. ZENITH-ANGLE DEPENDENCE OF ENERGY THRESHOLD AND FLUX SENSITIVITY

Figure 4 shows the sensitivity of the various IACT projects for small zenith angles ($\vartheta < 20^\circ$) just like it shows the EGRET sensitivity for on-axis observations. Both effective collection area A_{eff} and energy threshold E_{thr} of an IACT are to a good approximation proportional to $\cos^{-2}(\vartheta)$ as explained in the following.

The area perpendicular to the optical axis illuminated by the Cherenkov light at the position of the telescope is proportional to the square of the distance d to the shower maximum. d grows with ϑ as $d \propto 1/\cos(\vartheta)$. The energy threshold E_{thr} of a Cherenkov telescope is, for a given zenith angle, to a good approximation equivalent to a Cherenkov photon density threshold ρ_{thr} at the position of the telescope. ρ_{thr} is an instrumental constant determined by the trigger condition of the data acquisition system. The Cherenkov photon density ρ at the position of the telescope is a function of the primary Energy E and of the zenith angle ϑ . The dependence on the impact parameter can be neglected since we average over it. For a given primary energy, ρ decreases inversely proportional to the illuminated area, i.e. $\rho(E, \vartheta) \propto \cos^2(\vartheta)$. At least for electromagnetic showers, the atmosphere is (again to a good approximation) a linear calorimeter yielding a Cherenkov photon density directly proportional to the primary energy of the incident gamma photon, i.e. for a fixed ϑ we have $\rho(E, \vartheta) \propto E$. Hence, $\rho(E, \vartheta) \propto E \cdot \cos^2(\vartheta)$. It follows that to satisfy the trigger condition $\rho(E, \vartheta) > \rho_{\text{thr}}$, E has to increase with ϑ as $\cos^{-2}(\vartheta)$.

$$\begin{aligned} A_{\text{eff}}(\vartheta) &= A_{\text{eff}}(0^\circ) \cdot \cos^{-2}(\vartheta) \\ E_{\text{thr}}(\vartheta) &= E_{\text{thr}}(0^\circ) \cdot \cos^{-2}(\vartheta) \end{aligned} \quad (1.4)$$

The values for $E_{\text{thr}}(0^\circ)$ are shown in table 1.

An increase in effective collection area for gammas is accompanied by a proportional increase in hadronic background rate. The gain in flux sensitivity is therefore only the square-root of the gain in area:

$$F_{5\sigma}(E_{\text{thr}}(\vartheta), \vartheta) = F_{5\sigma}(E_{\text{thr}}(0^\circ), 0^\circ) \cdot \cos^{-1}(\vartheta) \quad (1.5)$$

where $F_{5\sigma}(E_{\text{thr}})$ is the integral flux above energy threshold E_{thr} which results in a 5σ detection after 50 h of observation time.

3.4. REQUIRED OBSERVATION TIME

Given an integral flux $F(E_{\text{thr}})$ above an energy threshold E_{thr} and a flux sensitivity expressed as $F_{5\sigma}(E_{\text{thr}})$ as defined in the previous section,

and assuming that the flux is so small that the signal is background dominated (the conservative assumption), we can calculate the observation time $T_{5\sigma}$ which is necessary to detect the flux with 5σ significance:

$$T_{5\sigma}(E_{\text{thr}}) = \left(\frac{F(E_{\text{thr}})}{F_{5\sigma}(E_{\text{thr}})} \right)^{-2} \cdot 50\text{h} \quad (1.6)$$

Cherenkov telescopes typically have a duty cycle of about 10 % due to the fact that they can only observe during good weather and at night (moon-less night for maximum sensitivity). This results typically in 1000 h of available observation time per year. For an individual source, rarely more than 100 h can be obtained.

4. THE AGENDA

Based on the observability criteria developed above, UNIDs can now be selected for an observation agenda. In the following, those sources are preselected which may be detected in less than 50 h of observation time. These are shown in tables 2, 3, 4, and 5 for further reference. The prime candidates are then selected requiring that a detection is possible even if the spectrum at 0.1 GeV is steeper than the nominal value by one standard deviation. The prime candidates are summarized in table 6. A discussion follows in section 5.

4.1. PRESELECTION

Using the formulae derived in section 3, tables 2, 3, 4, and 5 are compiled. All four tables have the same format. The tables are generated as follows: For each non-identified source of the third catalog and for each of the four IACT projects, the minimum zenith angle of observation ϑ_{min} is calculated using

$$\vartheta_{\text{min}} = |\phi - DEC| \quad (1.7)$$

and the corresponding minimum energy threshold $E_{\text{thr}}(\vartheta_{\text{min}})$ is determined according to equation 1.4. ϑ_{min} and the corresponding threshold are shown in the tables. If a source is not observable according to equation 1.3, it is omitted. Otherwise, the threshold is inserted into equation 1.1 to determine the extrapolated flux $F(E_{\text{thr}})$. From this flux, the necessary observation time $T_{5\sigma}$ is determined using equation 1.6. Flux and observation time together with the spectral index $\alpha(E_{\text{thr}})$ which the extrapolated spectrum would have at the IACT threshold, are also shown in the table. If $T_{5\sigma}$ is more than 50 h, the source is omitted.

In order to take into account the error of the EGRET spectral measurement and to explore a realistic worst case, the procedure is repeated

assuming an initial spectral index at 0.1 GeV which is larger by one standard deviation than the nominal value. The resulting modified values for $F(E_{\text{thr}})$, $\alpha(E_{\text{thr}})$ and $T_{5\sigma}$ are given in brackets after their nominal values. The modified value of $T_{5\sigma}$ is named $T'_{5\sigma}$ in the following.

For the case of VERITAS with its steep dependence of $F_{5\sigma}$ on E below 80 GeV (see figure 4), it turns out that for all sources the observation time can be reduced if the minimum threshold is raised to 80 GeV before entering the calculation. The table contains the values for this case.

After $T_{5\sigma}$ is calculated, the number of detected primary gamma photons is calculated conservatively assuming an effective collection area of 10^4 m^2 . If this number is smaller than 100, the value of $T_{5\sigma}$ is increased such that the number becomes equal to 100. This ensures that the source location can be determined with sufficiently high accuracy to improve the EGRET measurement. The values are marked if this correction was necessary.

4.2. PRIME CANDIDATES

Table 6 shows those sources from tables 2, 3, 4, and 5 which satisfy the additional restriction that the “modestly worst case” observation time $T'_{5\sigma}$ (see the previous section) is less than 50 h. These sources can be regarded as the prime candidates for allocating the valuable IACT observation time since only if a detection is possible, the EGRET location measurement can be improved. An upper limit on the flux value is only valuable if the observed object has been identified and models can be constrained.

5. DISCUSSION

The observability tables 2, 3, 4, and 5 and the selection of prime candidates in table 6 show that the next-generation IACTs may make a major contribution to the identification of EGRET UNIDs. Altogether 78 of them may be in the reach of the IACT sensitivity. Under the modest assumptions of spectral steepening made here, many sources may be detectable within few hours of observation time.

Among the 78 sources are 20 which have a tentative identification (given in the Third EGRET Catalog unless otherwise specified):

0010+7309 (SNR CTA1), 0241+6103 (LS I +61°303), 0617+2238 (SNR IC443), 0808+4844 (QSO 0809+483), 0812-0646 (PKS 0805-077), 0827-4247 (SNR Pup A) 0917+4427 (QSO 0917+449), 1009+4855 (QSO 1011+496), 1323+2200 (EQ 1324+224), 1410-6147 (SNR 312.4-00.4), 1627-2419 (rho Oph), 1800-2338 (SNR W 28), 1854-1514 (LS5039, a microquasar suggested by Paredes et al. (2000)), 1856+0114 (SNR W 44),

1903+0550 (SNR 040.4-00.5), 2020+4017 (SNR γ Cyg), 2100+6012 (4C 59.33), 2206+6602 (TXS 2206+650), 2255+1943 (QSO 2250+1926), and 2352+3752 (QSO 2346+385).

Some of these have already (unsuccessfully) been observed by present IACTs. They come as no surprise and will be included in observation schedules in any case since the known position of the possible counterpart makes the observation especially promising.

Among the 38 prime candidates shown in table 6, only 11 of the tentatively identified objects are present, mostly SNR candidates. Observers will face the additional problem here that these sources may be extended in angular size which may increase the necessary observation time. This is also true for all other UNIDs.

Increases in the required observation time will also arise in those few cases where θ_{95} , the radius of the 3EG position probability map, is near the radius of the IACT trigger field-of-view (typically $> 1^\circ$) and the true source position is accidentally on the boundary of the map. But most of the 78 selected UNIDs have a θ_{95} well below 1° (see tables 2, 3, 4, and 5).

A decrease in necessary observation time may be possible in case a candidate counterpart-pulsar is known. The IACT sensitivity can be greatly increased by introducing the known pulsar ephemeris into the analysis provided the emission is still pulsed at the IACT's threshold.

A nice opportunity to cross-calibrate all four IACT observatories are the prime candidate objects 1837-0606 and 1856+0114 (SNR W44?) which are observable from all four locations at similar zenith angles (see table 6).

In summary, the EGRET UNIDs are a promising field for the application of the next-generation IACTs. From the start of operations of the individual observatory it will probably take between 2 and 4 years until the between 16 and 27 prime candidates have been observed and analysed. This estimation takes into account that not the whole observation time will be dedicated to EGRET UNIDs. However, if the observatories cooperate and split the candidate list into four parts of 9 to 10 sources each, a coverage of all 38 prime candidates could be reached within one year since each observatory would only have to invest up to ≈ 500 h of observation time. The attempt to cover the remaining 40 non-prime candidates could equally be shared.

References

Arqueros, F., et al., 1999, in Kieda, D. et al. (eds.) Proc. "26th International Cosmic Ray Conference", 5, 215

- Barrio, J.A., et al., 1998, report MPI-PhE/98-5, Max-Planck-Institute for Physics, Munich
- de Jager, O.C., Harding, A.K., et al., 1996, *ApJ*, 457, 253
- D’Ettore Piazzoli, B., et al., 1999, in Kieda, D. et al. (eds.) Proc. “26th International Cosmic Ray Conference”, 2, 373
- Hartman, R.C., et al., 1999, *ApJ Suppl. Ser.*, 123, 79
- Hillas, A.M., et al., 1998, *ApJ*, 503, 744
- Hofmann, W., et al., 1999, in Dingus, B.L., et al. (eds.) Proc. “Towards a Major Atmospheric Cherenkov Detector VI”, AIP Proc. 515, 500
- Kaaret, P. & Cottam, J., 1996, *ApJ*, 462, L35
- Kataoka, J., et al., 1999, *ApJ*, 514, 138
- Krennrich, F., et al., 1999, in Dingus, B.L., et al. (eds.) Proc. “Towards a Major Atmospheric Cherenkov Detector VI”, AIP Proc. 515, 515
- Lamb, R.C. & Macomb, D.J., 1997, *ApJ*, 488, 872
- Lorenz, E., et al., 1999, in Dingus, B.L., et al. (eds.) Proc. “Towards a Major Atmospheric Cherenkov Detector VI”, AIP Proc. 515, 510
- McCullough, J.F., et al., 1999, in Kieda, D. et al. (eds.) Proc. “26th International Cosmic Ray Conference”, 2, 369
- Mori, M., et al., 1999, in Dingus, B.L., et al. (eds.) Proc. “Towards a Major Atmospheric Cherenkov Detector VI”, AIP Proc. 515, 485
- Mori, M., 2001, private communication
- Oser, S., et al., 1999, in Kieda, D. et al. (eds.) Proc. “26th International Cosmic Ray Conference”, 3, 464
- Paredes, J.M., et al., 2000, *Science*, 288, 2340
- Petry, D., 1997, PhD thesis, report MPI-PhE/97-27, Max-Planck-Institute for Physics, Munich
- Pühlhofer, G., et al., 1997, *Astropart. Phys.*, 8, 101
- Punch, M., et al., 1992, *Nature*, 358, 477
- Smith, D.A., et al., 1998, in Aubourg, E. et al. (eds.) Proc. “19th Texas Symposium on Relativistic Astrophysics”, *Nucl. Phys. B Proc.* 80
- Weekes, T.C., et al., 1989, *ApJ*, 342, 379
- Yadigaroglu, I.-A. & Romani, R.W., 1995, *ApJ*, 449, 211
- Zweerink, J.A., et al., 1999, in Kieda, D. et al. (eds.) Proc. “26th International Cosmic Ray Conference”, 5, 223

Table 2 Observability of unidentified and tentatively identified EGRET sources for project CANGAROO III

object name	3EG		CANGAROO III observability				
	θ_{95}^b [$^\circ$]	α^c	ϑ_{\min}^d [$^\circ$]	E_{thr}^e [GeV]	$F(E_{\text{thr}})^f$ [$\text{cm}^{-2}\text{s}^{-1}$]	$\alpha(E_{\text{thr}})^g$	$T_{5\sigma}^h$ [h]
0215+1123	1.06	1.03 ± 0.62	42	147	2.95E-11(3.21E-13)	1.48(2.10)	42(> 500)
0616-3310	0.63	1.11 ± 0.24	2	80	2.86E-11(5.74E-12)	1.41(1.65)	25(> 500)
0617+2238 ^a	0.13	1.01 ± 0.06	54	228	5.13E-11(3.22E-11)	1.46(1.52)	22(55)
0631+0642	0.46	1.06 ± 0.15	38	128	4.12E-11(1.41E-11)	1.51(1.66)	19(161)
0634+0521	0.67	1.03 ± 0.26	36	123	5.39E-11(8.47E-12)	1.48(1.74)	11(430)
0706-3837	0.90	1.30 ± 0.43	8	81	3.23E-11(1.81E-12)	1.60(2.03)	20(> 500)
0747-3412	0.70	1.22 ± 0.30	3	80	3.09E-11(4.16E-12)	1.52(1.82)	21(> 500)
0824-4610	0.61	1.36 ± 0.07	15	86	2.43E-11(1.51E-11)	1.66(1.73)	36(94)
0827-4247 ^a	0.77	1.10 ± 0.12	12	83	9.75E-11(4.35E-11)	1.40(1.52)	2.85 [‡] (11)
0841-4356	0.52	1.15 ± 0.09	13	84	1.14E-10(6.23E-11)	1.45(1.54)	2.43 [‡] (5.43)
0848-4429	0.62	1.05 ± 0.16	14	85	2.31E-10(7.87E-11)	1.35(1.51)	1.20 [‡] (3.53 [‡])
1014-5705	0.67	1.23 ± 0.20	26	99	4.73E-11(1.19E-11)	1.53(1.73)	11(175)
1027-5817	0.37*	0.94 ± 0.09	27	101	3.48E-10(1.87E-10)	1.39(1.48)	0.80 [‡] (1.49 [‡])
1048-5840	0.17	0.97 ± 0.09	28	102	2.62E-10(1.41E-10)	1.42(1.51)	1.06 [‡] (1.98 [‡])
1234-1318	0.76	1.09 ± 0.24	18	88	4.91E-11(9.63E-12)	1.39(1.63)	9.16(237)
1323+2200 ^a	0.47	0.86 ± 0.35	53	221	5.98E-11(4.04E-12)	1.31(1.66)	15(> 500)
1410-6147 ^a	0.36	1.12 ± 0.14	31	108	8.78E-11(3.30E-11)	1.57(1.71)	3.51(25)
1420-6038	0.32	1.02 ± 0.14	30	106	2.10E-10(7.91E-11)	1.47(1.61)	1.33 [‡] (4.24)
1627-2419 ^a	0.65	1.21 ± 0.27	7	81	2.67E-11(4.38E-12)	1.51(1.78)	28(> 500)
1631-4033	0.89	1.25 ± 0.27	10	82	2.24E-11(3.65E-12)	1.55(1.82)	41(> 500)
1655-4554	0.66	1.19 ± 0.24	15	86	4.63E-11(9.16E-12)	1.49(1.73)	9.99(255)
1704-4732	0.66	0.86 ± 0.33	17	87	1.29E-09(1.38E-10)	1.16(1.49)	0.22 [‡] (2.01 [‡])
1714-3857	0.51	1.30 ± 0.20	8	82	2.70E-11(7.06E-12)	1.60(1.80)	28(409)
1736-2908	0.62	1.18 ± 0.12	2	80	7.32E-11(3.28E-11)	1.48(1.60)	3.79 [‡] (19)
1741-2050	0.63	1.25 ± 0.12	10	83	2.05E-11(9.14E-12)	1.55(1.67)	49(247)
1744-3011	0.32	1.17 ± 0.08	1	80	9.72E-11(5.70E-11)	1.47(1.55)	2.86 [‡] (6.17)
1746-2851	0.13	0.70 ± 0.07	2	80	4.22E-09(2.64E-09)	1.00(1.07)	0.07 [‡] (0.11 [‡])
1800-2338 ^a	0.32	1.10 ± 0.10	7	81	1.46E-10(7.45E-11)	1.40(1.50)	1.91 [‡] (3.73 [‡])
1809-2328	0.16	1.06 ± 0.08	8	81	1.29E-10(7.57E-11)	1.36(1.44)	2.15 [‡] (3.67 [‡])
1812-1316	0.39	1.29 ± 0.11	18	88	2.65E-11(1.26E-11)	1.59(1.70)	31(139)
1824-1514	0.52	1.19 ± 0.18	16	86	4.18E-11(1.24E-11)	1.49(1.67)	12(141)
1826-1302	0.46	1.00 ± 0.11	18	88	2.78E-10(1.32E-10)	1.30(1.41)	1.00 [‡] (2.11 [‡])
1837-0606	0.19	0.82 ± 0.14	25	97	6.30E-10(2.40E-10)	1.12(1.26)	0.44 [‡] (1.16 [‡])
1850-2652	1.00	1.29 ± 0.45	4	80	6.08E-11(2.99E-12)	1.59(2.04)	5.44(> 500)
1856+0114 ^a	0.19	0.93 ± 0.10	32	112	3.33E-10(1.65E-10)	1.38(1.48)	0.83 [‡] (1.68 [‡])
1928+1733	0.75	1.23 ± 0.32	49	183	4.13E-11(3.74E-12)	1.68(2.00)	27(> 500)

For definitions see the end of table 5.

Table 3 Observability of unidentified and tentatively identified EGRET sources for project HESS I

object name	3EG		ϑ_{\min}^d [$^\circ$]	E_{thr}^e [GeV]	HESS I observability		$T_{5\sigma}^h$ [h]
	θ_{95}^b [$^\circ$]	α^c			$F(E_{\text{thr}})^f$ [$\text{cm}^{-2}\text{s}^{-1}$]	$\alpha(E_{\text{thr}})^g$	
0215+1123	1.06	1.03 ± 0.62	34	59	1.05E-10(2.02E-12)	1.33(1.95)	13(> 500)
0616-3310	0.63	1.11 ± 0.24	10	41	7.28E-11(1.72E-11)	1.41(1.65)	20(355)
0617+2238 ^a	0.13	1.01 ± 0.06	46	82	2.21E-10(1.48E-10)	1.31(1.37)	4.22(9.44)
0631+0642	0.46	1.06 ± 0.15	30	53	1.42E-10(5.53E-11)	1.36(1.51)	6.69(44)
0634+0521	0.67	1.03 ± 0.26	28	52	1.77E-10(3.49E-11)	1.33(1.59)	4.17(107)
0706-3837	0.90	1.30 ± 0.43	16	43	8.92E-11(6.57E-12)	1.60(2.03)	14(> 500)
0747-3412	0.70	1.22 ± 0.30	11	42	8.40E-11(1.38E-11)	1.52(1.82)	15(> 500)
0824-4610	0.61	1.36 ± 0.07	23	47	6.53E-11(4.24E-11)	1.66(1.73)	28(67)
0827-4247 ^a	0.77	1.10 ± 0.12	20	45	2.30E-10(1.11E-10)	1.40(1.52)	2.15(9.34)
0841-4356	0.52	1.15 ± 0.09	21	46	2.76E-10(1.59E-10)	1.45(1.54)	1.53(4.61)
0848-4429	0.62	1.05 ± 0.16	22	46	5.24E-10(1.96E-10)	1.35(1.51)	0.53 [‡] (3.04)
0859-4257	0.64	1.32 ± 0.20	20	45	5.09E-11(1.50E-11)	1.62(1.82)	44(> 500)
1014-5705	0.67	1.23 ± 0.20	34	58	1.07E-10(2.98E-11)	1.53(1.73)	13(166)
1027-5817	0.37 [*]	0.94 ± 0.09	35	60	6.67E-10(3.75E-10)	1.24(1.33)	0.42 [‡] (1.08)
1048-5840	0.17	0.97 ± 0.09	36	61	5.09E-10(2.86E-10)	1.27(1.36)	0.59(1.87)
1234-1318	0.76	1.09 ± 0.24	10	41	1.41E-10(3.33E-11)	1.39(1.63)	5.22(94)
1323+2200 ^a	0.47	0.86 ± 0.35	45	80	2.19E-10(2.11E-11)	1.16(1.51)	4.23(456)
1410-6147 ^a	0.36	1.12 ± 0.14	39	66	1.80E-10(7.28E-11)	1.42(1.56)	5.11(31)
1420-6038	0.32	1.02 ± 0.14	38	64	4.13E-10(1.67E-10)	1.32(1.46)	0.95(5.78)
1627-2419 ^a	0.65	1.21 ± 0.27	1	40	7.76E-11(1.54E-11)	1.51(1.78)	17(428)
1631-4033	0.89	1.25 ± 0.27	18	44	5.90E-11(1.14E-11)	1.55(1.82)	32(> 500)
1634-1434	0.49 [*]	1.15 ± 0.23	8	41	5.30E-11(1.33E-11)	1.45(1.68)	37(> 500)
1655-4554	0.66	1.19 ± 0.24	23	47	1.13E-10(2.57E-11)	1.49(1.73)	9.38(180)
1704-4732	0.66	0.86 ± 0.33	25	48	2.55E-09(3.32E-10)	1.16(1.49)	0.11 [‡] (1.11)
1714-3857	0.51	1.30 ± 0.20	16	43	7.44E-11(2.21E-11)	1.60(1.80)	20(224)
1717-2737	0.64	1.23 ± 0.15	5	40	5.19E-11(2.11E-11)	1.53(1.68)	38(229)
1719-0430	0.44	1.20 ± 0.24	18	44	4.87E-11(1.13E-11)	1.50(1.74)	47(> 500)
1736-2908	0.62	1.18 ± 0.12	6	40	2.01E-10(9.78E-11)	1.48(1.60)	2.53(11)
1741-2050	0.63	1.25 ± 0.12	2	40	6.28E-11(3.06E-11)	1.55(1.67)	26(108)
1744-3011	0.32	1.17 ± 0.08	7	41	2.63E-10(1.63E-10)	1.47(1.55)	1.48(3.88)
1746-2851	0.13	0.70 ± 0.07	6	40	8.36E-09(5.49E-09)	1.00(1.07)	0.03 [‡] (0.05 [‡])
1800-2338 ^a	0.32	1.10 ± 0.10	1	40	3.93E-10(2.16E-10)	1.40(1.50)	0.71 [‡] (2.17)
1809-2328	0.16	1.06 ± 0.08	0	40	3.40E-10(2.10E-10)	1.36(1.44)	0.88(2.29)
1810-1032	0.39 [*]	1.29 ± 0.16	12	42	6.17E-11(2.35E-11)	1.59(1.75)	28(193)
1812-1316	0.39	1.29 ± 0.11	10	41	8.91E-11(4.59E-11)	1.59(1.70)	13(49)
1824-1514	0.52	1.19 ± 0.18	8	41	1.28E-10(4.34E-11)	1.49(1.67)	6.28(55)
1826-1302	0.46	1.00 ± 0.11	10	41	7.49E-10(3.86E-10)	1.30(1.41)	0.37 [‡] (0.72 [‡])

continued on the next page

Table 3 (part 2) Observability of unidentified and tentatively identified EGRET sources for project HESS I

object name	3EG		ϑ_{\min}^d [$^\circ$]	E_{thr}^e [GeV]	HESS I observability		
	θ_{95}^b [$^\circ$]	α^c			$F(E_{\text{thr}})^f$ [$\text{cm}^{-2}\text{s}^{-1}$]	$\alpha(E_{\text{thr}})^g$	$T_{5\sigma}^h$ [h]
1837-0606	0.19	0.82 ± 0.14	17	44	1.54E-09(6.59E-10)	1.12(1.26)	$0.18^\ddagger(0.42^\ddagger)$
1850-2652	1.00	1.29 ± 0.45	4	40	1.83E-10(1.23E-11)	1.59(2.04)	$3.03(> 500)$
1856+0114 ^a	0.19	0.93 ± 0.10	24	48	9.55E-10(5.15E-10)	1.23(1.33)	$0.29^\ddagger(0.54^\ddagger)$
1928+1733	0.75	1.23 ± 0.32	41	69	1.99E-10(2.46E-11)	1.53(1.85)	4.42(290)
1958+2909	0.57	0.85 ± 0.20	52	106	2.48E-10(6.17E-11)	1.30(1.50)	4.36(71)

For definitions see the end of table 5.

Table 4 Observability of unidentified and tentatively identified EGRET sources for project MAGIC I

object name	3EG		ϑ_{\min}^d [$^\circ$]	E_{thr}^e [GeV]	MAGIC I observability		
	θ_{95}^b [$^\circ$]	α^c			$F(E_{\text{thr}})^f$ [$\text{cm}^{-2}\text{s}^{-1}$]	$\alpha(E_{\text{thr}})^g$	$T_{5\sigma}^h$ [h]
0010+7309 ^a	0.24	0.85 ± 0.10	44	58	7.87E-10(4.16E-10)	1.15(1.25)	$0.35^\ddagger(0.67^\ddagger)$
0215+1123	1.06	1.03 ± 0.62	18	33	2.27E-10(6.22E-12)	1.33(1.95)	$1.23^\ddagger(> 500)$
0229+6151	0.49	1.29 ± 0.18	33	43	7.07E-11(2.38E-11)	1.59(1.77)	8.17(72)
0241+6103 ^a	0.18	1.21 ± 0.07	32	42	2.15E-10(1.41E-10)	1.51(1.58)	$1.29^\ddagger(2.01)$
0323+5122	0.55	1.38 ± 0.41	22	35	3.67E-11(3.32E-12)	1.68(2.09)	$25(> 500)$
0348+3510	0.74	1.16 ± 0.27	6	30	7.70E-11(1.65E-11)	1.46(1.73)	4.91(108)
0426+1333	0.45 [*]	1.17 ± 0.25	15	32	8.09E-11(1.91E-11)	1.47(1.72)	4.74(85)
0439+1555	0.92	1.27 ± 0.44	13	32	1.44E-10(1.14E-11)	1.57(2.01)	$1.93^\ddagger(233)$
0510+5545	0.71	1.19 ± 0.20	27	38	8.72E-11(2.66E-11)	1.49(1.69)	4.75(51)
0613+4201	0.57	0.92 ± 0.26	13	32	2.26E-10(5.07E-11)	1.22(1.48)	$1.23^\ddagger(12)$
0617+2238 ^a	0.13	1.01 ± 0.06	6	30	8.11E-10(5.75E-10)	1.31(1.37)	$0.34^\ddagger(0.48^\ddagger)$
0628+1847	0.57	1.30 ± 0.10	10	31	6.96E-11(3.92E-11)	1.60(1.70)	6.13(19)
0631+0642	0.46	1.06 ± 0.15	22	35	2.49E-10(1.03E-10)	1.36(1.51)	$1.12^\ddagger(3.15)$
0634+0521	0.67	1.03 ± 0.26	24	36	2.89E-10(6.26E-11)	1.33(1.59)	$0.96^\ddagger(8.75)$
0808+4844 ^a	0.72	1.15 ± 0.45	20	34	6.47E-11(4.71E-12)	1.45(1.90)	$7.76(> 500)$
0812-0646 ^a	0.72	1.34 ± 0.29	36	46	3.12E-11(5.29E-12)	1.64(1.93)	$45(> 500)$
0910+6556	0.86	1.20 ± 0.26	37	47	5.07E-11(1.02E-11)	1.50(1.76)	18(430)
0917+4427 ^a	0.56	1.19 ± 0.14	15	32	7.10E-11(3.16E-11)	1.49(1.63)	6.15(31)
1009+4855 ^a	0.75 [*]	0.90 ± 0.37	20	34	1.48E-10(1.71E-11)	1.20(1.57)	$1.88^\ddagger(112)$

continued on the next page

Table 4 (part 2) Observability of unidentified and tentatively identified EGRET sources for project MAGIC I

object name	3EG				MAGIC I observability		
	θ_{95}^b [$^\circ$]	α^c	ϑ_{\min}^d [$^\circ$]	E_{thr}^e [GeV]	$F(E_{\text{thr}})^f$ [$\text{cm}^{-2}\text{s}^{-1}$]	$\alpha(E_{\text{thr}})^g$	$T_{5\sigma}^h$ [h]
1234-1318	0.76	1.09 ± 0.24	42	55	9.48E-11(2.09E-11)	1.39(1.63)	5.86(121)
1323+2200 ^a	0.47	0.86 ± 0.35	7	30	6.71E-10(9.07E-11)	1.16(1.51)	0.41 [‡] (3.56)
1337+5029	0.72	0.83 ± 0.29	21	35	3.50E-10(6.42E-11)	1.13(1.42)	0.79 [‡] (8.07)
1631-1018	0.72	1.20 ± 0.27	39	50	3.19E-11(5.96E-12)	1.50(1.77)	47(> 500)
1719-0430	0.44	1.20 ± 0.24	34	43	5.09E-11(1.19E-11)	1.50(1.74)	16(294)
1736-2908	0.62	1.18 ± 0.12	58	108	4.67E-11(2.02E-11)	1.63(1.75)	47(253)
1744-3011	0.32	1.17 ± 0.08	59	114	5.64E-11(3.21E-11)	1.62(1.70)	35(107)
1746-2851	0.13	0.70 ± 0.07	58	106	3.16E-09(1.94E-09)	1.15(1.22)	0.09 [‡] (0.14 [‡])
1800-2338 ^a	0.32	1.10 ± 0.10	53	82	1.45E-10(7.42E-11)	1.40(1.50)	3.71(14)
1809-2328	0.16	1.06 ± 0.08	52	81	1.31E-10(7.64E-11)	1.36(1.44)	4.55(13)
1810-1032	0.39*	1.29 ± 0.16	40	50	4.60E-11(1.70E-11)	1.59(1.75)	23(167)
1812-1316	0.39	1.29 ± 0.11	42	55	5.66E-11(2.83E-11)	1.59(1.70)	16(66)
1824+3441	0.82	1.03 ± 0.50	6	30	4.05E-10(2.33E-11)	1.33(1.83)	0.69 [‡] (54)
1824-1514	0.52	1.19 ± 0.18	44	58	7.48E-11(2.38E-11)	1.49(1.67)	10(99)
1826-1302	0.46	1.00 ± 0.11	42	54	5.22E-10(2.61E-10)	1.30(1.41)	0.53 [‡] (1.06 [‡])
1835+5918	0.15	0.69 ± 0.07	30	40	4.50E-09(2.96E-09)	0.99(1.06)	0.06 [‡] (0.09 [‡])
1837-0423	0.52	1.71 ± 0.44	33	43	4.44E-11(3.08E-12)	2.01(2.45)	21(> 500)
1837-0606	0.19	0.82 ± 0.14	35	45	1.50E-09(6.38E-10)	1.12(1.26)	0.19 [‡] (0.44 [‡])
1850-2652	1.00	1.29 ± 0.45	56	95	4.64E-11(2.12E-12)	1.59(2.04)	43(> 500)
1856+0114 ^a	0.19	0.93 ± 0.10	28	38	1.26E-09(6.97E-10)	1.23(1.33)	0.22 [‡] (0.40 [‡])
1903+0550 ^a	0.64	1.38 ± 0.17	23	35	9.10E-11(3.35E-11)	1.68(1.85)	4.12(30)
1928+1733	0.75	1.23 ± 0.32	11	31	6.75E-10(1.07E-10)	1.53(1.85)	0.41 [‡] (2.60)
1958+2909	0.57	0.85 ± 0.20	0	30	1.07E-09(3.43E-10)	1.15(1.35)	0.26 [‡] (0.81 [‡])
2016+3657	0.55	1.09 ± 0.11	8	31	3.43E-10(1.83E-10)	1.39(1.50)	0.81 [‡] (1.52 [‡])
2020+4017 ^a	0.16	1.08 ± 0.04	11	31	1.26E-09(1.00E-09)	1.38(1.42)	0.22 [‡] (0.28 [‡])
2021+3716	0.30	0.86 ± 0.10	8	31	2.18E-09(1.23E-09)	1.16(1.26)	0.13 [‡] (0.23 [‡])
2022+4317	0.72	1.31 ± 0.19	14	32	6.47E-11(2.16E-11)	1.61(1.80)	7.34(66)
2027+3429	0.77	1.28 ± 0.15	6	30	8.77E-11(3.72E-11)	1.58(1.73)	3.78(21)
2033+4118	0.28	0.96 ± 0.10	12	31	1.47E-09(8.26E-10)	1.26(1.36)	0.19 [‡] (0.34 [‡])
2035+4441	0.54	1.08 ± 0.26	16	32	2.83E-10(6.29E-11)	1.38(1.64)	0.98 [‡] (7.85)
2046+0933	0.60*	1.22 ± 0.51	19	34	8.42E-11(4.33E-12)	1.52(2.03)	4.57(> 500)
2100+6012 ^a	0.48	1.21 ± 0.25	31	41	6.33E-11(1.41E-11)	1.51(1.76)	9.84(199)
2206+6602 ^a	0.88	1.29 ± 0.26	37	47	3.87E-11(7.80E-12)	1.59(1.85)	30(> 500)
2227+6122	0.46	1.24 ± 0.14	32	42	1.06E-10(4.55E-11)	1.54(1.68)	3.59(20)
2248+1745	0.94	1.11 ± 0.39	11	31	1.11E-10(1.18E-11)	1.41(1.80)	2.51 [‡] (215)
2255+1943 ^a	0.87*	1.36 ± 0.61	9	31	1.30E-10(3.93E-12)	1.66(2.27)	2.14 [‡] (> 500)
2314+4426	0.78	1.34 ± 0.32	15	32	8.74E-11(1.38E-11)	1.64(1.96)	4.06(164)
2352+3752 ^a	0.94	1.47 ± 0.68	9	31	4.18E-11(8.50E-13)	1.77(2.45)	17(> 500)

For definitions see the end of table 5.

Table 5 Observability of unidentified and tentatively identified EGRET sources for project VERITAS

object name	3EG				VERITAS observability		
	θ_{95}^b [°]	α^c	ϑ_{\min}^d [°]	E_{thr}^e [GeV]	$F(E_{\text{thr}})^f$ [cm ⁻² s ⁻¹]	$\alpha(E_{\text{thr}})^g$	$T_{5\sigma}^h$ [h]
0010+7309 ^a	0.24	0.85 ± 0.10	41	141	2.70E-10(1.31E-10)	1.30(1.40)	1.03 [‡] (2.12 [‡])
0215+1123	1.06	1.03 ± 0.62	21	91	5.86E-11(8.55E-13)	1.33(1.95)	4.74 [‡] (> 500)
0229+6151	0.49	1.29 ± 0.18	30	106	1.63E-11(4.65E-12)	1.74(1.92)	25(308)
0241+6103 ^a	0.18	1.21 ± 0.07	29	105	5.34E-11(3.28E-11)	1.66(1.73)	5.20 [‡] (8.47 [‡])
0348+3510	0.74	1.16 ± 0.27	3	80	1.86E-11(3.06E-12)	1.46(1.73)	15 [‡] (> 500)
0426+1333	0.45*	1.17 ± 0.25	18	89	1.83E-11(3.34E-12)	1.47(1.72)	17(497)
0439+1555	0.92	1.27 ± 0.44	16	87	2.95E-11(1.51E-12)	1.57(2.01)	9.41 [‡] (> 500)
0510+5545	0.71	1.19 ± 0.20	24	96	2.18E-11(5.52E-12)	1.49(1.69)	13 [‡] (196)
0613+4201	0.57	0.92 ± 0.26	10	82	7.02E-11(1.22E-11)	1.22(1.48)	3.96 [‡] (34)
0617+2238 ^a	0.13	1.01 ± 0.06	9	82	2.20E-10(1.47E-10)	1.31(1.37)	1.26 [‡] (1.89 [‡])
0628+1847	0.57	1.30 ± 0.10	13	84	1.40E-11(7.14E-12)	1.60(1.70)	27(104)
0631+0642	0.46	1.06 ± 0.15	25	98	6.16E-11(2.19E-11)	1.36(1.51)	4.51 [‡] (13)
0634+0521	0.67	1.03 ± 0.26	27	100	7.34E-11(1.22E-11)	1.48(1.74)	3.78 [‡] (42)
0808+4844 ^a	0.72	1.15 ± 0.45	17	87	1.64E-11(7.80E-13)	1.45(1.90)	20(> 500)
0910+6556	0.86	1.20 ± 0.26	34	116	1.27E-11(2.03E-12)	1.65(1.91)	45(> 500)
0917+4427 ^a	0.56	1.19 ± 0.14	12	84	1.71E-11(6.67E-12)	1.49(1.63)	18(118)
1009+4855 ^a	0.75*	0.90 ± 0.37	17	87	4.74E-11(3.87E-12)	1.20(1.57)	5.86 [‡] (365)
1234-1318	0.76	1.09 ± 0.24	45	162	1.96E-11(3.33E-12)	1.54(1.78)	26(> 500)
1323+2200 ^a	0.47	0.86 ± 0.35	10	82	2.11E-10(2.01E-11)	1.16(1.51)	1.32 [‡] (14 [‡])
1337+5029	0.72	0.83 ± 0.29	18	89	1.21E-10(1.68E-11)	1.13(1.42)	2.30 [‡] (20)
1800-2338 ^a	0.32	1.10 ± 0.10	56	251	2.61E-11(1.19E-11)	1.55(1.65)	23(110)
1809-2328	0.16	1.06 ± 0.08	55	249	2.47E-11(1.32E-11)	1.51(1.59)	26(89)
1824+3441	0.82	1.03 ± 0.50	3	80	1.11E-10(3.92E-12)	1.33(1.83)	2.50 [‡] (326)
1826-1302	0.46	1.00 ± 0.11	45	160	1.19E-10(5.31E-11)	1.45(1.56)	2.33 [‡] (5.24 [‡])
1835+5918	0.15	0.69 ± 0.07	27	101	1.80E-09(1.11E-09)	1.14(1.21)	0.15 [‡] (0.25 [‡])
1837-0606	0.19	0.82 ± 0.14	38	129	4.41E-10(1.62E-10)	1.27(1.41)	0.63 [‡] (1.72 [‡])
1856+0114 ^a	0.19	0.93 ± 0.10	31	108	3.48E-10(1.73E-10)	1.38(1.48)	0.80 [‡] (1.61 [‡])
1903+0550 ^a	0.64	1.38 ± 0.17	26	99	1.62E-11(5.00E-12)	1.68(1.85)	24(249)
1928+1733	0.75	1.23 ± 0.32	14	85	1.45E-10(1.67E-11)	1.53(1.85)	1.92 [‡] (19)
1958+2909	0.57	0.85 ± 0.20	3	80	3.47E-10(9.10E-11)	1.15(1.35)	0.80 [‡] (3.05 [‡])
2016+3657	0.55	1.09 ± 0.11	5	81	8.92E-11(4.27E-11)	1.39(1.50)	3.11 [‡] (6.50 [‡])
2020+4017 ^a	0.16	1.08 ± 0.04	8	82	3.34E-10(2.55E-10)	1.38(1.42)	0.83 [‡] (1.09 [‡])
2021+3716	0.30	0.86 ± 0.10	5	81	7.08E-10(3.62E-10)	1.16(1.26)	0.39 [‡] (0.77 [‡])
2022+4317	0.72	1.31 ± 0.19	11	83	1.38E-11(3.86E-12)	1.61(1.80)	27(349)
2027+3429	0.77	1.28 ± 0.15	2	80	1.88E-11(6.91E-12)	1.58(1.73)	15 [‡] (105)
2033+4118	0.28	0.96 ± 0.10	9	82	4.37E-10(2.24E-10)	1.26(1.36)	0.64 [‡] (1.24 [‡])
2035+4441	0.54	1.08 ± 0.26	13	84	7.58E-11(1.32E-11)	1.38(1.64)	3.67 [‡] (30)
2046+0933	0.60*	1.22 ± 0.51	22	94	1.78E-11(5.45E-13)	1.52(2.03)	18(> 500)

continued on the next page

Table 5 (part 2) Observability of unidentified and tentatively identified EGRET sources for project VERITAS

object name	3EG		ϑ_{\min}^d [$^\circ$]	E_{thr}^e [GeV]	VERITAS observability		
	θ_{95}^b [$^\circ$]	α^c			$F(E_{\text{thr}})^f$ [$\text{cm}^{-2}\text{s}^{-1}$]	$\alpha(E_{\text{thr}})^g$	$T_{5\sigma}^h$ [h]
2100+6012 ^a	0.48	1.21 ± 0.25	28	103	1.57E-11(2.77E-12)	1.66(1.91)	26(> 500)
2227+6122	0.46	1.24 ± 0.14	29	105	2.56E-11(9.65E-12)	1.69(1.83)	11 [‡] (71)
2248+1745	0.94	1.11 ± 0.39	14	85	2.69E-11(1.93E-12)	1.41(1.80)	10 [‡] (> 500)
2255+1943 ^a	0.87*	1.36 ± 0.61	12	84	2.46E-11(4.06E-13)	1.66(2.27)	11 [‡] (> 500)
2314+4426	0.78	1.34 ± 0.32	12	84	1.83E-11(2.12E-12)	1.64(1.96)	16(> 500)

^a The object has already been tentatively identified in 3EG (Hartman et al. 1999).

^b The radius of the 95% confidence contour in the position probability map in 3EG.

^c The integral spectral index at 0.1 GeV (see equ. 1.1) with statistical error from 3EG.

^d The minimum zenith angle, see equ. 1.7.

^e The IACTs minimum energy threshold for this source, see equ. 1.4.

^f The expected flux at the minimum energy threshold, see equ. 1.1; in brackets the flux which is obtained from an extrapolation using an initial spectrum at 0.1 GeV steeper by one standard deviation.

^g The integral spectral index at the IACTs minimum energy threshold for this source, see equ. 1.1; in brackets the index obtained if the spectrum at 0.1 GeV was steeper by one standard deviation.

^h The observation time to obtain a detection with 5σ significance; in brackets the observation time necessary if the spectrum at 0.1 GeV was steeper by one standard deviation.

* The shape of the position probability map is irregular (see 3EG).

‡ The detection is photon flux limited: the observation time was increased such that 100 gammas are detected.

Table 6 The prime candidates for EGRET-UNID observations by the next-generation Imaging Cherenkov Telescopes

3EG name	tentative ID	$\vartheta_{\min}(\text{C})^a$ [$^\circ$]	$\vartheta_{\min}(\text{H})^b$ [$^\circ$]	$\vartheta_{\min}(\text{M})^c$ [$^\circ$]	$\vartheta_{\min}(\text{V})^d$ [$^\circ$]
0010+7309	SNR CTA 1	-	-	44	41
0241+6103	LSI+61 $^\circ$ 303	-	-	32	29
0613+4201	-	-	-	13	10
0617+2238	SNR IC443	-	46	6	9
0628+1847	-	-	-	10	-
0631+0642	-	-	30	22	25
0634+0521	-	-	-	24	27
0827-4247	SNR Pup A	12	20	-	-
0841-4356	-	13	21	-	-
0848-4429	-	14	22	-	-
0917+4427	QSO 0917+449	-	-	15	-
1027-5817	-	27	35	-	-
1048-5840	-	28	36	-	-
1323+2200	EQ 1324+224	-	-	7	10
1337+5029	-	-	-	21	18
1410-6147	SNR 312.4-00.4	31	39	-	-
1420-6038	-	30	38	-	-
1704-4732	-	17	25	-	-
1736-2908	-	2	6	-	-
1744-3011	-	1	7	-	-
1746-2851	-	2	6	58	-
1800-2338	SNR W 28	7	1	53	-
1809-2328	-	8	0	52	-
1812-1316	-	-	10	-	-
1826-1302	-	18	10	42	45
1835+5918	-	-	-	30	27
1837-0606	-	25	17	35	38
1856+0114	SNR W 44	32	24	28	31
1903+0550	SNR 040.5-00.5	-	-	23	-
1928+1733	-	-	-	11	14
1958+2909	-	-	-	0	3
2016+3657	-	-	-	8	5
2020+4017	SNR γ Cyg	-	-	11	8
2021+3716	-	-	-	8	5
2027+3429	-	-	-	6	-
2033+4118	-	-	-	12	9
2035+4441	-	-	-	16	13
2227+6122	-	-	-	32	-

^a the minimum zenith angle for observations with CANGAROO III

^b the minimum zenith angle for observations with HESS I

^c the minimum zenith angle for observations with MAGIC I

^d the minimum zenith angle for observations with VERITAS